

# DC-Biased Optical OFDM for IM/DD Passive Optical Network Systems

M. F. Sanya, L. Djogbe, A. Vianou, and C. Aupetit-Berthelemot

**Abstract**—In the context of access networks, orthogonal frequency division multiplexing (OFDM) has been extensively studied for fiber-based optical communications. A DC-biased optical OFDM (DCO-OFDM) scheme (where no real constellation or Hermitian symmetry constraint is used), is proposed and explored for the first time, to the best of our knowledge, in an intensity modulated and direct detected (IM/DD) passive optical network (PON). In this paper, an analysis of the peak-to-average-power ratio and a discussion of the algorithm complexity are investigated. By means of numerical simulation in 12 Gb/s next-generation (NG)-PON1 OFDM with a split ratio of 1:64 users and 35 km reach, the new DCO-OFDM method is shown to achieve the same performance as the well-known conventional DCO-OFDM but with less computational complexity (gain of almost 54.3% on the required operations per bit). As a result, the new DCO-OFDM seems very interesting and a good candidate for NG-PON cost-sensitive applications, considering the implementation of real-time demonstrators including digital modulators and demodulators based on digital signal processing or a field-programmable gate array (FPGA).

**Index Terms**—Computational complexity; IM/DD fiber link; OFDM; Passive optical access networks.

## I. INTRODUCTION

The explosive growth of bandwidth-intensive applications imposed a challenge on the last mile broadband access network, which needs low cost, higher capacity, and better flexibility. Due to this, service providers have to look for a new technology as solutions to deploy new applications. Telecommunication interest groups, such as the Full Service Access Network (FSAN), the Institute of Electrical and Electronics Engineers (IEEE), and the International Telecommunication Union (ITU), have proposed the next-generation passive optical network (NG-PON). The first step (NG-PON1) allows the use of the existing Giga-PON optical distribution network (ODN) to control cost, and it is defined as an asymmetric

10 G system (rates of 10 Gb/s downstream and 2.5 Gb/s upstream) with a split ratio of 64 over conventional 20 km (maximum reach of 60 km) with an optical budget between 28 and 31 dB and the possibility to use forward error coding [FEC: Reed–Solomon (248, 232)]. The basic requirements for NG-PON2 were for a system with at least 40 Gb/s and 40 km of reach at a 64-way split. No backward compatibility with existing NG-PON1 is required. Between the proposed solutions, in 2012 time- and wavelength-division multiplexing (TWDM)-PON was retained [1]. Beyond this second phase, modulation formats with higher spectral efficiency than non-return-to-zero (NRZ) are planned, such as code division multiple access (CDMA), wavelength-division multiplexing (WDM) and multicarrier modulations [like orthogonal frequency division multiplexing (OFDM)] [2]. Optical OFDM (O-OFDM) solutions can be broadly divided into two types: one using intensity modulation (IM) and the other using linear field modulation. Future generations of communications networks must meet three requirements: to provide ever-increasing user rates at limited costs of infrastructure deployment [capital expenditure (CapEx)] and energy consumption [operational expenditure (OpEx)]. That is why, in optical access networks, IM and direct detection (IM/DD) systems [3] coupled with the use of the single-mode fiber (SMF) widely installed all around the world are preferred [4]. In IM/DD optical systems, the intensity of the optical carrier is modulated by the electrical signal. The fast Fourier transform (FFT) and its inverse fast Fourier transform (IFFT) are key components of OFDM systems. In intensity modulated systems, the signal should be real and positive. Then, some conditions must be imposed on the OFDM subcarrier data so that the IFFT operation produces a real signal. Usually, one uses Hermitian symmetry [2,5] for which double-sized (I)FFT components are required. For example,  $2N$ -point (I)FFT transforms are needed to modulate  $N$  frequency symbols. It is well known [6] that to improve system performance it is necessary to increase FFT size and bit precision. However, in the context of optical gigabit-per-second (Gb/s) transmissions, the complexity of an (I)FFT may become a challenge. As OFDM transceivers operating at 10 Gb/s require highly optimized DSP blocks, it is interesting to propose a cost-sensitive solution with fewer resources that reduces the system computational complexity. For this reason, several solutions have been proposed [7–9]. One was the use of a discrete Hartley transform (DHT) OFDM technique [7] where only real constellations such as binary phase-shift keying (BPSK) or pulse amplitude modulation (PAM) can be applied to obtain real OFDM

Manuscript received November 4, 2014; revised January 27, 2015; accepted January 27, 2015; published March 11, 2015 (Doc. ID 226149).

M. F. Sanya (e-mail: frejus.sanya@ensil.unilim.fr) is with XLIM Laboratory, UMR CNRS 7252, University of Limoges, 123 Avenue Albert-Thomas, 87060 Limoges, France. He is also with LETIA Laboratory at EPAC/UAC in Benin.

L. Djogbe and A. Vianou are with LETIA Laboratory at the Polytechnic School of the Abomey-Calavi University of Benin, 01 BP 2009, Cotonou, Benin.

C. Aupetit-Berthelemot is with XLIM Laboratory, UMR CNRS 7252, University of Limoges, 123 Avenue Albert-Thomas, 87060 Limoges, France. <http://dx.doi.org/10.1364/JOCN.7.000205>

signals. Other methods use the modified FFT algorithms for a real-valued sequence when computing the discrete Fourier transform (DFT) of complex-valued data [10]. Recently, position modulation OFDM (PM-OFDM) was proposed, in the context of optical wireless communications, to produce a real signal from the complex IFFT output in the transmitter using additional processing [8]. Two signals corresponding to the real and the imaginary parts of the IFFT output are produced. Then, positive and negative parts of each signal are further separated into two, resulting in four real signals in total, which are then sequentially transmitted. More recently, an approach similar to PM-OFDM, but without the additional separation of the positive and negative portions [9], was proposed with asymmetrically clipped optical OFDM (ACO-OFDM) for an additive white Gaussian noise (AWGN) flat channel link without a cyclic prefix (CP). It consists of generating a conventional complex OFDM signal and juxtaposing the real and imaginary parts in the time domain to obtain a real OFDM signal. But, to the best of the authors' knowledge, the performance of this last method [9] has not yet been analyzed in the context of PON transmissions taking into account realistic component models.

In this paper, our goal is to implement this last method for DC-biased optical OFDM (DCO-OFDM) [11,12] in IM/DD PON systems. We will call that "New DCO-OFDM" throughout the paper. To the best of our knowledge, this is the first time that this method is presented with further discussion in terms of computational complexity for a realistic chirped optical channel model [13], as shown in Fig. 1. Here, a CP is inserted into each OFDM symbol to combat the chromatic dispersion of the fiber link. Simulations are performed thanks to VPItransmissionMaker Optical Systems, taking into account optoelectronic device models issued from experimental characterizations of the French ANR EPOD project to which we contributed. The New DCO-OFDM scheme will be compared with the conventional technique in which Hermitian symmetry is used [2,12].

The paper is organized as follows: in Section II, an overview of the conventional DCO-OFDM is provided, followed by a short review of the New DCO-OFDM approach. A general discussion in terms of peak-to-average power ratio (PAPR) and computational complexity is provided in Section III for both optical conventional DCO-OFDM and New DCO-OFDM. Section IV presents the modeling of each component in the transmission link after presentation of

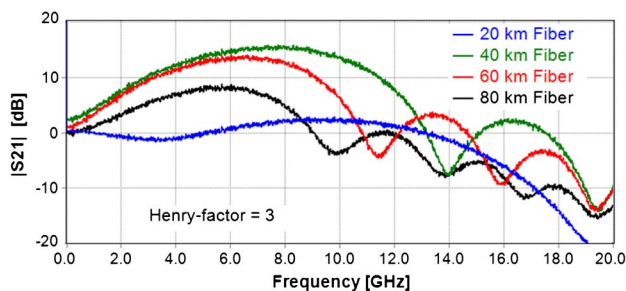


Fig. 1. Channel frequency response variation versus fiber length of the simulated link considering a DFB laser Henry factor of 3.

the simulated IM/DD fiber link. Performance analysis and discussion are given in Section V. The bit error rate (BER) performance is first presented for the case of a flat channel with AWGN in terms of the normalized optical energy-per-bit to noise ratio and then for the real PON channel link in terms of photodiode received optical power and reached transmission distance. Optical split ratio ( $1 \times M$ ) loss is taken into account to consider the number  $M$  of users [optical network units (ONUs)] that share the same physical medium (optical fiber). Finally, our conclusions are given in Section VI.

## II. DC-BIASED OPTICAL OFDM SCHEMES

In this section, an overview of the conventional DCO-OFDM method is presented followed by a description of the proposed New DCO-OFDM.

### A. Conventional DCO-OFDM

Generally, to generate real OFDM signals, the frequency symbols  $X(k)$  at the  $2N$ -IFFT block input are constrained to have Hermitian symmetry:

$$X(2N - k) = X^*(k), \quad k = 1, 2, \dots, N - 1, \quad (1)$$

where  $X(0) = X(N) = 0$ , and  $X^*(k)$  is the complex conjugation of  $X(k)$ . To get a positive and real OFDM signal in IM/DD systems, two methods are often used after the IFFT output signal given by

$$x(n) = \sum_{k=0}^{2N-1} X(k) \exp\left(j2\pi \frac{kn}{2N}\right). \quad (2)$$

One is DCO-OFDM and the other is ACO-OFDM [14,15], which is not investigated in this paper.

In DCO-OFDM [5,16], a certain bias value is added to the resulting real signal at the IFFT output and then all the remaining negative values are clipped at zero. Usually, a DC-bias value of 7 dB is used [2].

The DC value increases the transmitter power requirement and the clipping induces clipping noise in both the even and odd subcarriers [2,12]. In general, a CP is inserted into each OFDM symbol to combat channel dispersion. A typical block diagram of conventional DCO-OFDM is shown in Fig. 2.

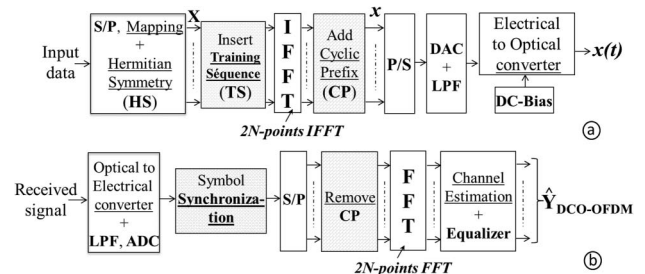


Fig. 2. Block diagram of a conventional DCO-OFDM scheme: (a) transmitter and (b) receiver.

In Fig. 2, the input data are parallelized and mapped using a multilevel quadrature amplitude modulation (M-QAM) constellation. The resulting signal is fed into an IFFT block, after Hermitian symmetry, to create a real signal. A CP is appended and a training sequence (TS) is added as a header of the OFDM frames. The signal is analogically converted and properly biased (DC component) before driving the electrical-to-optical converter. The resulting optical signal is transmitted into the channel. At the receiver side, after detection by an optical-to-electrical converter, the resulting received signal is analog-to-digital converted and synchronized. Finally, the signal is demodulated (CP-removal and FFT operation) and then equalized after channel estimation.

### B. New DCO-OFDM

One drawback of the previously described method is the use of Hermitian symmetry inducing the need of  $2N$ -point (IFFT) size. A scheme with  $N$ -point (IFFT) size that allows a real OFDM signal without Hermitian symmetry [9] is proposed to be tested in the PON context. In this case, it is well known that the IM/DD channel frequency response is not flat due to the impact of interaction between phase and intensity modulation in the laser and chromatic dispersion of the optical fiber, such as demonstrated in [13] and presented in Fig. 1. The new approach consists of directly applying the symbols  $X(k)$  at the input of an  $N$ -point IFFT block, resulting in a time complex OFDM signal [Eq. (3)] that can also be expressed by Eq. (4), considering that  $X(0)$  is set to zero in order to avoid any DC shift:

$$x(n) = \sum_{k=0}^{N-1} X(k) \exp\left(j2\pi \frac{kn}{N}\right). \quad (3)$$

$$x(n) = x_R(n) + jx_I(n), \quad n = 0, 1, \dots, N-1. \quad (4)$$

Here,  $x_R(n)$  and  $x_I(n)$  are, respectively, the real and imaginary parts of  $x(n)$ . A CP of length  $N_{CP} = N \cdot \text{CP}$  is appended at the  $N$ -point IFFT output, resulting in signal  $x_{CP}(n)$  with length  $N' = N + N_{CP}$ , where CP is the CP ratio in percent. The transmitted signal  $x_t(n')$  is obtained by juxtaposing in the time domain both the  $N'$  real and  $N'$  imaginary parts of  $x_{CP}(n)$ , as shown in Fig. 3, where  $n' = 0, 1, \dots, 2N' - 1$ . Then, a proper DC-biasing is done as in a conventional DCO-OFDM transmitter, after insertion of a  $2N'$ -length TS as a header of the OFDM frames. At the receiver side (Fig. 4), after accurate symbol synchronization, each  $2N'$  received real signal sample  $y(n')$  is separated into two different signal components of length  $N'$ . Then a CP removal block is appended, followed by an  $N$ -point FFT computation before demodulation as in conventional complex OFDM systems.

In practice, as  $N'$  grows large (i.e.,  $N' \geq 64$ ), the central limit amplitude of the complex OFDM signal  $x_{CP}(n)$  can be modeled as a Gaussian random variable with zero mean and a variance  $\sigma^2 = E\{x_{CP}^2(n)\}$  [17]. Thus, both the amplitudes of the real and imaginary parts of  $x_{CP}(n)$  can also be

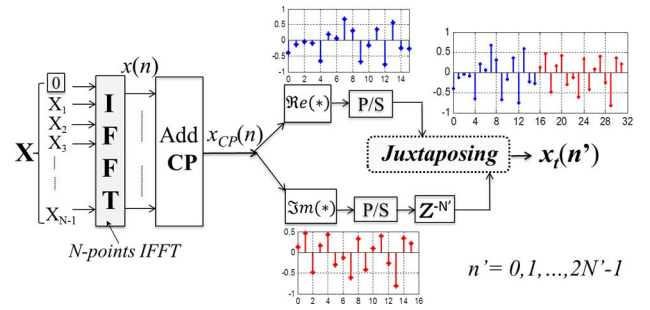


Fig. 3. Transmitter block diagram of the proposed technique including an example of real with imaginary signals and overall transmitted time signal  $x_t(n')$ .

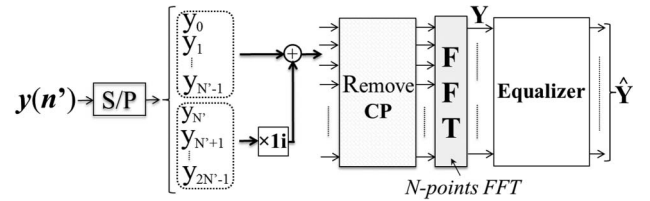


Fig. 4. Receiver block diagram of the New DCO-OFDM.

approximated by Gaussian distributions with zero mean and variance  $\sigma^2/2$ . Therefore according to Eq. (5), variance  $\sigma_1^2$  of the New DCO-OFDM signal is also half of the complex time signal variance  $\sigma^2$ .

Moreover, as the length of the OFDM frame is doubled while the IFFT/FFT block size is reduced by half, the spectral efficiency of the New DCO-OFDM is the same as the conventional real DCO-OFDM scheme. The following paragraph explains this, without considering the CP for simplification. Spectral efficiency is defined as the number of information bits per unit bandwidth. Suppose that  $N$  information symbols are transmitted and the number of bits per symbol is the same for all the schemes. Due to Hermitian symmetry, in the conventional real DCO-OFDM,  $2N$  subcarriers should be used to transmit  $N$  information symbols ( $2N$ -length channel). For the New DCO-OFDM, since Hermitian symmetry is not required, the  $N$ -length channel is used two times to transmit  $N$  information symbols (as both the real and imaginary parts of the information symbols are time interleaved). Therefore, spectral efficiencies of the two DCO-OFDM schemes are the same.

In this paper, for fair comparison, the New DCO-OFDM scheme with (IFFT) size of  $N$  will be compared with the conventional DCO-OFDM scheme with  $2N$ -point (IFFT):

$$\begin{aligned} \sigma_1^2 &= \frac{1}{2N'} \sum_{k=0}^{2N'-1} |x_t(k')|^2 \\ &= \frac{1}{2} \left\{ \left( \frac{1}{N'} \sum_{k=0}^{N'-1} [|x_t(k')|^2] \right) + \left( \frac{1}{N'} \sum_{k=N'}^{2N'-1} [|x_t(k')|^2] \right) \right\} \\ &= \frac{1}{2} \left\{ \frac{\sigma^2}{2} + \frac{\sigma^2}{2} \right\} = \frac{\sigma^2}{2}. \end{aligned} \quad (5)$$

### III. PAPR AND COMPUTATIONAL COMPLEXITY

In this section, we discuss the PAPR and computational complexity of the described conventional DCO-OFDM and New DCO-OFDM.

#### A. PAPR Comparison

One of the important disadvantages of OFDM modulation is its important PAPR. The PAPR of a discrete OFDM signal is defined as the ratio of the maximum peak power to the average power over each OFDM symbol:

$$\text{PAPR}\{x(n)\} = \frac{\max(|x(n)|^2)}{E\{|x(n)|^2\}}, \quad n = 0, 1, \dots, N-1. \quad (6)$$

Indeed, the fact that data carried by different subcarriers can be independent induces a high probability of the appearance of large peaks in the time domain of the OFDM signal. As in optical fiber communications, the power of an OFDM signal is amplified by a driver before modulating the laser, and the largest peaks of the signal are always clipped due to amplifier saturation. For a fixed saturation power and a fixed input power of the amplifier, when the PAPR increases, the clipping probability also increases. The signal clipping induces in-band noise that degrades the signal-to-noise ratio (SNR) and out-of-band radiation that causes interchannel interference. For this reason, the average OFDM signal power must be adjusted so that the signal is rarely clipped.

To study PAPR characteristics of OFDM modulation, the complementary cumulative distribution function (CCDF) is usually used to find the clipping probability of the signal. The CCDF function is defined as the probability that a PAPR exceeds a given value  $\text{PAPR}_\epsilon$ , as described by

$$\text{PAPR} = \Pr(\text{PAPR} > \text{PAPR}_\epsilon). \quad (7)$$

Figure 5 shows the CCDF of both studied DCO-OFDM modulation formats. It is seen that the proposed technique presents similar CCDF as the conventional DCO-OFDM, resulting in no PAPR increase. This can be justified by visualizing (as shown in Fig. 5) the probability density functions (PDFs) of both generated DCO-OFDM signals, which present two Gaussians with the same mean value, and almost the same maximum and variance.

#### B. Computational Complexity

In OFDM transmission, the inverse and DFT operations are performed efficiently using a FFT algorithm. An (I)FFT of size  $2N$  requires approximately  $4 \cdot (2N) \cdot \log_2(2N)$  real operations (multiplications plus additions) [18]. For the conventional DCO-OFDM scheme, the number of real operations required per second for the transmitter is computed:

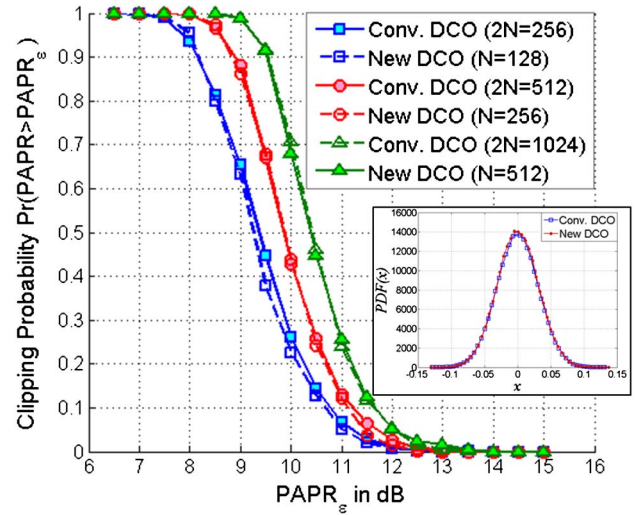


Fig. 5. CCDF comparison of conventional DCO-OFDM and New DCO-OFDM for different (I)FFT sizes. A PDF function of both conventional and New DCO-OFDM signals is shown for easier interpretation.

$$N_{\text{ConvDCO}}^{\text{Tx}} = 4 \cdot (2N) \cdot \frac{\log_2(2N)}{T_{\text{OFDM}}}, \quad (8)$$

with  $T_{\text{OFDM}}$  being the period of each transmitted OFDM sample. According to Fig. 2(a), this is given by

$$T_{\text{OFDM}} = 2N \cdot (1 + \text{CP}) \cdot T_S, \quad (9)$$

where CP is the CP ratio in percent, and  $T_S$  is the M-QAM symbol period as shown in

$$T_S = T_b \cdot \log_2(M), \quad (10)$$

where  $T_b$  is the time representing one information bit.

At the receiver side, we need to take into account the complex single tap equalizer on each subcarrier used. As only half of the subcarriers in conventional DCO-OFDM are used due to the Hermitian symmetry of Eq. (1) with the zeroth and  $N$ th subcarriers set to zero (to avoid any DC shift), if we assume that the complex multiplications are implemented with the usual four real multiplications and two real additions [18], the number of real operations required per second for the conventional DCO-OFDM receiver will be

$$N_{\text{ConvDCO}}^{\text{Rx}} = \frac{[4 \cdot (2N) \cdot \log_2(2N) + 6 \cdot (N-1)]}{T_{\text{OFDM}}}. \quad (11)$$

According to Fig. 3 of the New DCO-OFDM scheme, each transmitted OFDM sample has period of twice (because of the juxtaposition) the obtained OFDM symbol period at the  $N$ -point IFFT given by

$$T'_{\text{OFDM}} = 2 \cdot [N \cdot (1 + \text{CP}) \cdot T_S]. \quad (12)$$

Since the IFFT inputs are used excepting the zeroth subcarrier (set to zero), the number of real operations

required per second for both the transmitter and receiver of the New DCO-OFDM are, respectively, given by

$$N_{\text{NewDCO}}^{\text{Tx}} = 4 \cdot (N) \cdot \frac{\log_2(N)}{T_{\text{OFDM}}^v}, \quad (13)$$

$$N_{\text{NewDCO}}^{\text{Rx}} = \frac{[4 \cdot (N) \cdot \log_2(N) + 6 \cdot (N - 1)]}{T_{\text{OFDM}}^v}. \quad (14)$$

By combining Eqs. (9) and (10) with Eqs. (8) and (11), the overall complexity order in real operations per bit is given for the transmitter [Eq. (15)] and the receiver [Eq. (16)] blocks of conventional DCO-OFDM:

$$O_{\text{ConvDCO}}^{\text{Tx}} = T_b \cdot N_{\text{ConvDCO}}^{\text{Tx}} = \frac{4 \cdot \log_2(2N)}{(1 + \text{CP}) \cdot \log_2(M)}, \quad (15)$$

$$O_{\text{ConvDCO}}^{\text{Rx}} = O_{\text{ConvDCO}}^{\text{Tx}} + \frac{3 \cdot (N - 1)}{N \cdot (1 + \text{CP}) \cdot \log_2(M)}. \quad (16)$$

The same procedure is done by inserting Eqs. (10) and (12) into Eqs. (13) and (14). This gives, for the New DCO-OFDM scheme, an overall complexity order in real operations per bit of Eq. (17) for transmitter and Eq. (18) for receiver blocks:

$$O_{\text{NewDCO}}^{\text{Tx}} = T_b \cdot N_{\text{NewDCO}}^{\text{Tx}} = \frac{2 \cdot \log_2(N)}{(1 + \text{CP}) \cdot \log_2(M)}, \quad (17)$$

$$O_{\text{NewDCO}}^{\text{Rx}} = O_{\text{NewDCO}}^{\text{Tx}} + \frac{3 \cdot (N - 1)}{N \cdot (1 + \text{CP}) \cdot \log_2(M)}. \quad (18)$$

Using Eqs. (15)–(18), the total number of operations required per bit ( $O^{\text{Tx+Rx}}$ ) (transmitter and receiver) in both DCO-OFDM schemes is

$$O_{\text{ConvDCO}}^{\text{Tx+Rx}} = \frac{[8 \cdot (N) \cdot \log_2(2N) + 3 \cdot (N - 1)]}{N(1 + \text{CP}) \cdot \log_2(M)}, \quad (19)$$

$$O_{\text{NewDCO}}^{\text{Tx+Rx}} = \frac{[4 \cdot (N) \cdot \log_2(N) + 3 \cdot (N - 1)]}{N(1 + \text{CP}) \cdot \log_2(M)}. \quad (20)$$

Let us define  $G(N)$  as the computational complexity per bit savings when using New DCO-OFDM instead of conventional DCO-OFDM. This is computed for any CP value used and M-QAM constellation size by

$$G(N) = \left\{ \left[ 1 - \left( \frac{[4 \cdot (N) \cdot \log_2(N) + 3 \cdot (N - 1)]}{[8 \cdot (N) \cdot \log_2(2N) + 3 \cdot (N - 1)]} \right) \right] \times 100 \right\} \%. \quad (21)$$

According to Fig. 6, it can be seen that the computational complexity per bit savings  $G(N)$  decreases slightly with the (I)FFT size but is at least 52.2% for  $N = 4096$  ( $2N = 8192$ ) and 54.3% for  $N = 64$  ( $2N = 128$ ). Hence, a gain of up to

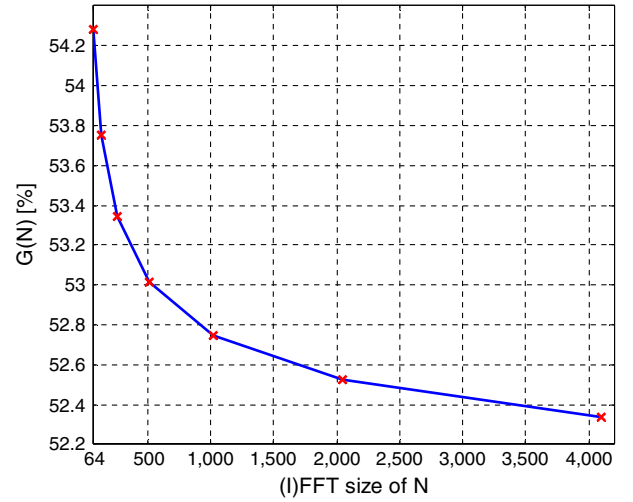


Fig. 6. Computational complexity per bit savings  $G(N)$  as function of (I)FFT size.

54.3% in terms of computational complexity per bit can be reached with the New DCO-OFDM compared to conventional DCO-OFDM.

#### IV. TRANSMISSION LINK MODEL

This section presents the simulated 12 Gb/s PON IM/DD fiber link (Fig. 7), in which a variable optical attenuator (VOA) is used to emulate an optical budget, as in PON systems given a fixed optical split ratio loss. Neither in-line optical amplification nor chromatic dispersion compensation is considered. The frequency response of the simulated link (Fig. 7) is shown in Fig. 1. A bias-tee is used for fixing the appropriate polarization point of the emitter according to the generated real OFDM signal power. The resulting (Tx) signal is directly modulated with a 1550 nm 1915 LMA analog distributed feedback (DFB) laser. Then the optical signal is sent through a standard single-mode fiber (SSMF) before being detected at the receiver side by a PIN transimpedance amplifier (TIA) photodiode following the demodulation step.

The link parameters are summarized in Table I. A CP of 1.56% is considered. 4QAM constellations are used. Zero-forcing channel equalization is used with knowledge by the receiver of a certain number of OFDM training symbols. In practice, signal synchronization is important. Specifically, Schmidl and Cox’s algorithm is generally used

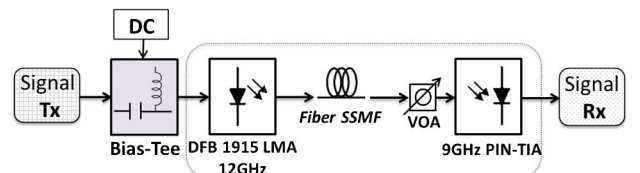


Fig. 7. Simulated IM/DD PON link.

TABLE I  
OPTICAL CHANNEL PARAMETERS

Parameter	Value
Laser threshold current	18 mA
Laser bias current	60 mA
Laser bandwidth & slope efficiency	12 GHz
Laser slope efficiency	0.2 W/A
Laser chirp	3.0
Laser RIN	-160 dB/Hz
Laser driver transconductance	1/50 (A/V)
Photodiode PIN responsivity @ 1550 nm	0.85 A/W
PIN-TIA 3 dB bandwidth	9 GHz
Photodiode transimpedance	750 $\Omega$
Photodiode dark current	1 nA
Photodiode thermal noise	18 pA/Hz <sup>1/2</sup>
SSMF nonlinear coefficient	$3.0 \times 10^{-20}$ m <sup>2</sup> /W
SSMF chromatic dispersion @ 1550 nm	17 ps/(km · nm)
SSMF attenuation coefficient	0.2 dB/km
SSMF core area	$80 \times 10^{-12}$ m <sup>2</sup>

[19,20]. This algorithm finds an approximate starting point of the OFDM symbol by using a TS in which the first half is identical to the second one in the time domain. A variation of this algorithm is used in [20,21]. The timing synchronization technique is based on the autocorrelation properties with use of special tailored TS [21] to estimate the beginning of the received OFDM symbol. A timing metric (as defined in [19]) is used and location of the peak position is utilized for symbol timing synchronization. For our design, similar real-valued time-domain TS, as in [21], is used for the conventional DCO-OFDM and the same  $2N$ -length TS (before the CP process) is added in front of the OFDM transmitted time signal in the New DCO-OFDM. Both OFDM modulator and demodulator blocks are operated off-line and implemented with MATLAB, resulting in signal (Tx) generation at the transmitter side and signal (Rx) processing at the receiver side. The power at the input of the optical fiber is 9.2 dBm. The BER performance is theoretically estimated from the SNR  $\approx \frac{1}{(\text{EVM})^2}$  via the measured error vector magnitude [22] by

$$\text{BER} = 4 \cdot \left( 1 - \frac{1}{2 \left[ 2^{\frac{\log_2(M)}{2}} - 1 \right]} \right) Q \left[ \sqrt{\left( \frac{2 \cdot \text{SNR}}{P} \right)} \right], \quad (22)$$

where  $Q$  is the  $Q$ -function,  $P$  is the average symbol power of the constellation, and  $P = (n_F)^2$  can be found in Table II with  $n_F$  being the constellation normalization factor [23]. Equation (22) is given in [23] for general square and cross QAM constellations. A direct Monte Carlo (MC) error counting simulation is also carried out for comparison with Eq. (22) in Fig. 8.

The DFB laser model is described with rate equations as in [13] where the relation between the instantaneous frequency  $\nu(t)$  and the optical modulation power  $P(t)$  is shown by

$$\nu(t) = \nu_0 + \Delta\nu(t) = \frac{\alpha}{4\pi} \left( \frac{1}{P(t)} \frac{dP(t)}{dt} + \kappa P(t) \right), \quad (23)$$

TABLE II  
NORMALIZATION FACTORS FOR DIFFERENT  
CONSTELLATIONS

Constellation	(Bits/Symbol)	$n_F$
BPSK	1	1
QPSK/4QAM	2	$\sqrt{2}$
Cross 8-QAM	3	$\sqrt{6}$
16QAM	4	$\sqrt{10}$
Cross 32QAM	5	$\sqrt{20}$
64QAM	6	$\sqrt{42}$
Cross 128QAM	7	$\sqrt{82}$
256QAM	8	$\sqrt{170}$
Cross 512QAM	9	$\sqrt{330}$
1024QAM	10	$\sqrt{682}$

$$\Delta\nu(t) = \frac{1}{2\pi} \frac{d\phi(t)}{dt}, \quad (24)$$

where  $\alpha$  is the laser Henry factor,  $\kappa$  is the adiabatic chirp factor, and  $\phi(t)$  is the phase modulation. The optical signal propagation through the SSMF can be described by the nonlinear Schrödinger equation given by Eq. (25) and numerically resolved with the symmetrically split-step Fourier method [24]:

$$\frac{\partial A}{\partial z} = -\frac{j}{2} \beta_2 \frac{\partial^2 A}{\partial t^2} - \frac{\alpha_1}{2} A + j\gamma |A|^2 A, \quad (25)$$

where  $\beta_2$  (s<sup>2</sup>/m) is the dispersion parameter,  $\alpha_1$  (dB/km) is the fiber attenuation coefficient, and  $\gamma$  (m<sup>2</sup>/W) is the fiber nonlinearity coefficient.

At the receiver side, the photodetector is modeled by a PIN photodiode with its TIA. Both shot and thermal noise associated with the detection process are taken into account as in [25].

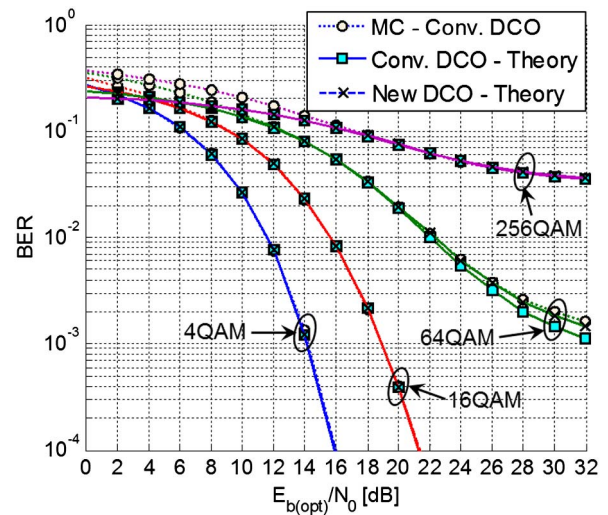


Fig. 8. BER performance versus  $E_{b(\text{opt})}/N_0$  of the conventional DCO-OFDM (Conv. DCO, IFFT size of 1024) and the New DCO-OFDM (New DCO, IFFT size of 512) for different QAM constellations using theoretical BER calculation. A MC error counting simulation is carried out for conventional DCO.

## V. RESULTS AND DISCUSSION

In this section, we present results obtained for both the conventional and New DCO-OFDM schemes in the case of a flat channel with AWGN in terms of the normalized optical energy-per-bit to noise ratio and then for a simulated PON channel link (Fig. 1). For fair comparison,  $N$ -point (IFFT) blocks are used with the New DCO-OFDM scheme while  $2N$ -point (IFFT) blocks are employed with the conventional one. For example, New DCO-OFDM with  $N = 512$  should be compared to conventional DCO-OFDM with  $2N = 1024$ .

### A. Performance in an AWGN Flat Channel

Before we start with the result obtained in a realistic chirped optical channel link, we first draw the BER performance of the two DCO-OFDM modulation formats as a function of the normalized optical energy-per-bit to noise power for different QAM constellations and (IFFT) sizes of 512 and 1024 for, respectively, New DCO-OFDM and conventional DCO-OFDM.

According to [9,17], the average transmitted optical power is one of the main constraints in optical systems. Thus, in order to study the optical power efficiency of optical systems, the normalized optical energy-per-bit to noise power is usually used. By setting the emitted optical power to unity for both DCO-OFDM signals, we observe in Fig. 8 that the New DCO-OFDM presents similar BER performance as the conventional DCO-OFDM for all simulated M-QAM constellations. BER estimations are also carried out for conventional DCO-OFDM through MC error counting. It can be seen that the theoretical expression using Eq. (22) shows similar BER values to those obtained by error counting simulation. Therefore, we choose to use the theoretical expression of Eq. (22) for BER performance estimation. As the New DCO-OFDM exhibits the same PAPR as the conventional DCO-OFDM (Fig. 5), the noted similar BER could be explained by the fact that, in the transmission, any noise distortion is spread over two consecutive blocks rather than one block in the New DCO-OFDM. This induces the same overall SNR compared with conventional DCO-OFDM at the receiver side. Similar results are obtained in [9] for the case of ACO-OFDM. Hence, we can start in the next section with the performance investigation in the case of a realistic channel link.

### B. Performance in a PON IM/DD Fiber Link

In the context of optical IM/DD transmission, we know that the interplay between the laser chirp and the chromatic dispersion of the fiber [13,26] results in attenuation dips in the channel frequency response (Fig. 1).

In order to ensure that Eq. (22) can be used with VPI simulations, some results are plotted in back-to-back with MC error counting in Fig. 9. As expected, all the curves obtained with the theoretical method are fairly close to the

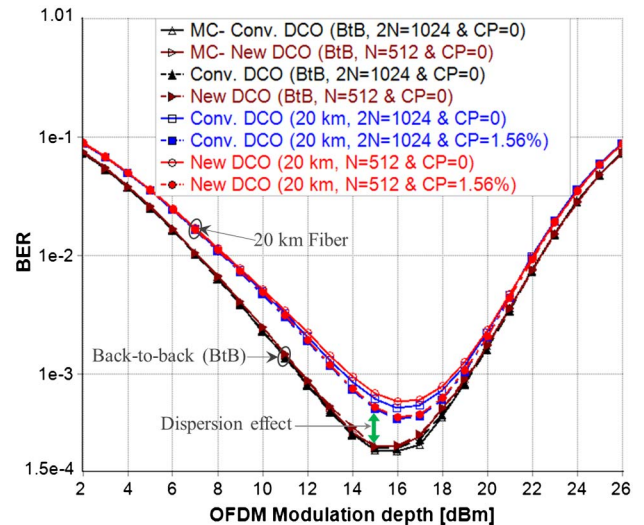


Fig. 9. BER versus modulation depth (OFDM signal power) of the conventional and New DCO-OFDM schemes in back-to-back (without dispersion) and 20 km fiber span at an optical budget of 28 dB and 4QAM constellation. A MC simulation is shown in back-to-back (BtB) for comparison with the theoretical method of Eq. (22).

MC results. This permits us to use Eq. (22) for BER estimation in VPI simulations. Indeed, BER performance in terms of the emitted signal modulation depth for a given polarization point of the laser (60 mA) is presented in Fig. 9. An optical budget of 28 dB (NG-PON1 Class B+) and a 20 km fiber span are considered for both DCO-OFDM schemes. It is seen that the BER performance of the New DCO-OFDM is very close to the conventional method. For example, the received RF spectra are also similar (Fig. 10).

The results of Fig. 9 are used to choose a well-adapted bias current coupled to the appropriated signal power in order to avoid or reduce any distortion induced by the hard clipping and nonlinear characteristic of the laser. For example, to satisfy a BER of  $10^{-3}$  (with the use of FEC), it can be seen that RF power of 13.7 dBm is needed to reach 20 km distance with an optical budget of 28 dB.

In addition, the BER performance can be improved when an optimal OFDM modulation depth is used (Fig. 9). In our design, this optimal RF power is observed at a value of 16 dBm. For the highest power, the clipping noise and laser nonlinearity characteristic penalize the transmission. In that case, the laser is modulated beyond the linear area

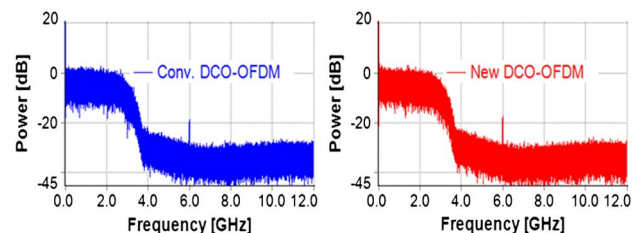


Fig. 10. RF spectrum in the positive side band of the conventional and New DCO-OFDM signals for 4QAM constellation, 20 km fiber span, and optical budget of 28 dB.

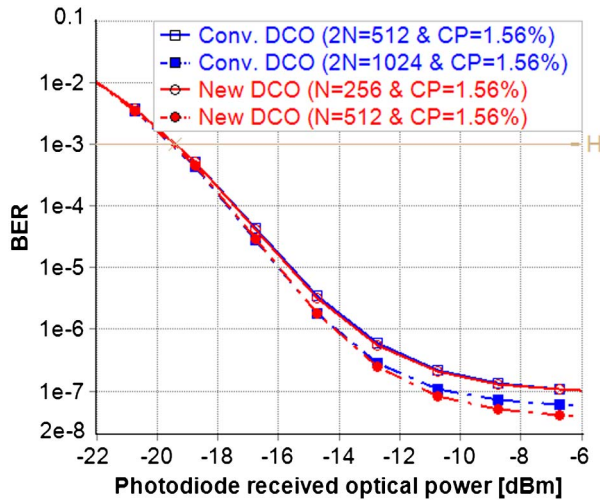


Fig. 11. BER versus received optical power and FFT size of the conventional and New DCO-OFDM signals for 4QAM constellation and 20 km fiber span.

of its power characteristic [5]. Moreover, back-to-back performance (without dispersion) is shown and compared with results obtained for 20 km fiber (Fig. 9). As we can see, a BER penalty [5] is observed between the back-to-back performance results and after 20 km transmission. This BER penalty is induced by chromatic dispersion of the fiber [26] and can be slightly reduced with the use of CP to reach better BER values. We present in Figs. 11 and 12 the BER versus the received optical power for different FFT and CP sizes. Results obtained confirm that the performance in New DCO-OFDM is very close to that of conventional DCO-OFDM. This could result from the fact that some clipping noise or distortion is spread over two blocks in the New DCO-OFDM rather than one block in conventional DCO-OFDM. That could be considered an implicit “MIMO-like” coding in the New DCO-OFDM scheme. In

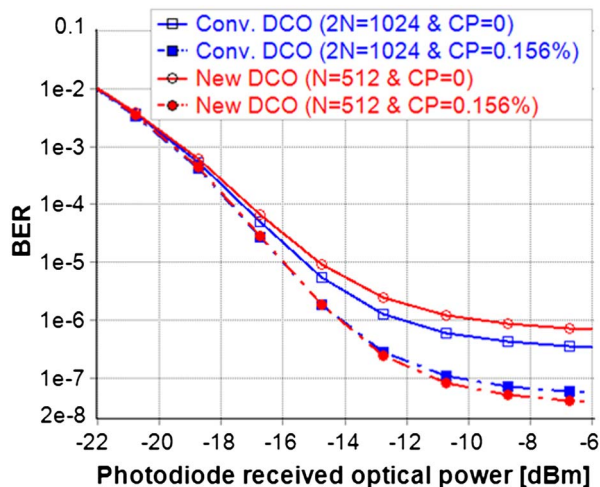


Fig. 12. BER versus received optical power and CP size of the conventional and New DCO-OFDM signals for 4QAM constellation and 20 km fiber span.

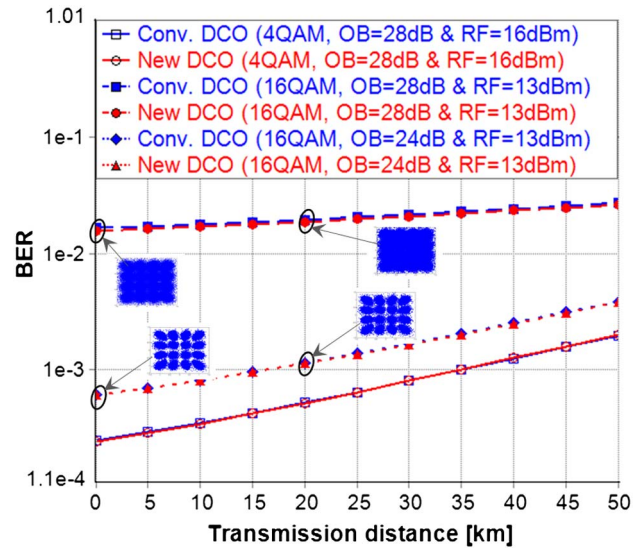


Fig. 13. BER versus transmission distance of the conventional and New DCO-OFDM signal for 4/16QAM constellations with specific optical budget (OB) and optimized RF power values at  $2N = 1024$  and  $CP = 1.56\%$ .

addition, from the results of Fig. 12 when increasing the size of the CP by 1.56%, it is shown that New DCO-OFDM gives slightly better performance than the conventional one. As an example, the BER is improved by more than one decade with a received optical power higher than  $-12$  dBm, whereas it is less than one decade for the conventional method.

In a PON context, both distance and power budget are usually considered. To satisfy a BER of  $10^{-3}$ , results of Fig. 13 show that it is possible with the two methods to reach 35 km transmission distance with a 28 dB optical budget (split ratio of 64 users). Thus we demonstrate that halving the FFT size by using New DCO-OFDM is possible while maintaining the performance. An example is also shown in Fig. 13 when using 16-QAM constellation. We can see that, for 16QAM constellation with an optimized RF value of 13 dBm, the BER performance of conventional and New DCO-OFDM are similar and better at  $OB = 24$  dB than when  $OB = 28$  dB is used (see Fig. 13 constellations). This can be justified by the SNR gap observed in Fig. 8, where for a fixed BER, 16QAM modulation is more subjected to distortion than 4QAM.

## VI. CONCLUSION

The performance of the New DCO-OFDM scheme is analyzed in both an AWGN flat channel and a chirped realistic IM/DD PON fiber link. Compared with the well-known conventional DCO-OFDM, it is shown that the New DCO-OFDM can achieve the same system performance in terms of the normalized optical energy-per-bit to noise power or data rate, distance transmission, and optical budget, but with fewer resources. Therefore, this New DCO-OFDM scheme, which permits dividing by 2 the required IFFT/FFT size, seems to be a good candidate for a PON O-OFDM

access scheme considering the significant simplification of the computational complexity associated with a possible reduction of the power consumption or chip area, particularly in the case of the development of specific processors [application-specific integrated circuits (ASICs)] of new transmitters. It has been demonstrated in this paper for a PON context that a 35 km transmission distance with 28 dB optical budget (split ratio of 64 users) and 12 Gb/s data rate is performed in an IM/DD fiber link with a gain of 53.1% on the required operations per bit (in both transmitter and receiver blocks) by New DCO-OFDM over conventional DCO-OFDM. In addition, this offers new advantages for known data-rate increase system techniques such as adaptive loading techniques [4,11,16] and ADO-OFDM [17].

#### ACKNOWLEDGMENTS

This work was supported by the SCAC of the French Embassy in Benin, the XLIM Laboratory, UMR CNRS 7252 in France, and LETIA Laboratory at EPAC/UAC in Benin and the Limousin region.

#### REFERENCES

- [1] Y. Luo, X. Zhou, F. Effenberger, X. Yan, G. Peng, Y. Qian, and Y. Ma, "Time- and wavelength-division multiplexed passive optical network (TWDM-PON) for next-generation PON stage 2 (NG-PON2)," *J. Lightwave Technol.*, vol. 31, no. 4, pp. 587–593, 2013.
- [2] J. Armstrong, "OFDM for optical communications," *J. Lightwave Technol.*, vol. 27, no. 3, pp. 189–204 2009.
- [3] R. Hu, Q. Yang, X. Xiao, T. Gui, Z. Li, M. Luo, S. Yu, and S. You, "Direct-detection optical OFDM superchannel for long-reach PON using pilot regeneration," *Opt. Express*, vol. 21, pp. 26513–26519, 2013.
- [4] T.-A. Truong, M. Arzel, H. Lin, B. Jahan, and M. Jezequel, "DFT precoded OFDM—An alternative candidate for next generation PONs," *J. Lightwave Technol.*, vol. 32, no. 6, pp. 1228–1238, Mar. 2014.
- [5] L. Zhou, N. Chand, X. Liu, G. Peng, H. Lin, Z. Li, Z. Wang, X. Zhang, S. Wang, and F. Effenberger, "Demonstration of software-defined flexible-PON with adaptive data rates between 13.8 Gb/s and 5.2 Gb/s supporting link loss budgets between 15 dB and 35 dB," in *European Conf. on Optical Communication (ECOC)*, Sept. 21–25, 2014.
- [6] R. Bouziane, P. A. Milder, R. J. Koutsoyannis, Y. Benlachtar, J. C. Hoe, M. Glick, and R. I. Killely, "Dependence of optical OFDM transceiver ASIC complexity on FFT size," in *Optical Fiber Communication Conf. and Expo. and the Nat. Fiber Optic Engineers Conf. (OFC/NFOEC)*, Mar. 4–8, 2012, pp. 1–3.
- [7] M. Moreolo, J. Fàbrega, F. Vilchez, L. Nadal, and G. Junyent, "Experimental demonstration of a cost-effective bit rate variable IM/DD optical OFDM with reduced guard band," *Opt. Express*, vol. 20, pp. B159–B164, 2012.
- [8] A. Nuwanpriya, A. Grant, S.-W. Ho, and L. Luo, "Position modulating OFDM for optical wireless communications," in *IEEE Workshop on Optical Wireless Communications*, Dec. 3–7, 2012, pp. 1219–1223.
- [9] F. Barrami, Y. Le Guennec, E. Novakov, J.-M. Duchamp, and P. Busson, "A novel FFT/IFFT size efficient technique to generate real time optical OFDM signals compatible with IM/DD systems," in *European Microwave Conf. (EuMC)*, Oct. 6–10, 2013, pp. 1247–1250.
- [10] H. V. Sorensen, D. L. Jones, M. Heideman, and C. S. Burrus, "Real-valued fast Fourier transform algorithms," *IEEE Trans. Acoust. Speech Signal Process.*, vol. 35, no. 6, pp. 849–863, June 1987.
- [11] M. Zhang and Z. Zhang, "An optimum DC-biasing for DCO-OFDM system," *IEEE Commun. Lett.*, vol. 18, no. 8, pp. 1351–1354, Aug. 2014.
- [12] M. F. Sanya, C. Aupetit-Berthelemot, L. Djogbe, and A. Vianou, "D-C ACO-OFDM and DCO-OFDM for passive optical network: Performance comparison in IM/DD fiber link," in *23rd Wireless and Optical Communication Conf. (WOCC)*, May 9–10, 2014.
- [13] L. A. Neto, D. Erasme, N. Genay, P. Chanclou, Q. Deniel, F. Traore, T. Anfray, R. Hmadou, and C. Aupetit-Berthelemot, "Simple estimation of fiber dispersion and laser chirp parameters using the downhill simplex fitting algorithm," *J. Lightwave Technol.*, vol. 31, no. 2, pp. 334–342, Jan. 2013.
- [14] M. F. Sanya, C. Aupetit-Berthelemot, L. Djogbe, and A. Vianou, "Performance analysis of known unipolar optical OFDM techniques in PON IM/DD fiber link," in *Int. Conf. on High Capacity Optical Networks and Enabling Technologies (HONET-CNS)*, Dec. 11–13, 2013, pp. 184–188.
- [15] M. F. Sanya, C. Aupetit-Berthelemot, L. Djogbe, and A. Vianou, "Diversity-combining in asymmetrically clipped optical OFDM for PON IM/DD fiber link," in *IEEE Int. Conf. on Communications Workshops (ICC)*, June 10–14, 2014, pp. 403–406.
- [16] D. Bykhovsky and S. Arnon, "An experimental comparison of different bit-and-power-allocation algorithms for DCO-OFDM," *J. Lightwave Technol.*, vol. 32, no. 8, pp. 1559–1564, Apr. 2014.
- [17] S. D. Dissanayake and J. Armstrong, "Comparison of ACO-OFDM, DCO-OFDM and ADO-OFDM in IM/DD systems," *J. Lightwave Technol.*, vol. 31, no. 7, pp. 1063–1072, Apr. 2013.
- [18] S. G. Johnson and M. Frigo, "A modified split-radix FFT with fewer arithmetic operations," *IEEE Trans. Signal Process.*, vol. 55, no. 1, pp. 111–119, Jan. 2007.
- [19] T. M. Schmidl and D. C. Cox, "Robust frequency and timing synchronization for OFDM," *IEEE Trans. Commun.*, vol. 45, no. 12, pp. 1613–1621, Dec. 1997.
- [20] L. Nadal, M. Svaluto Moreolo, J. M. Fabrega, A. Dochhan, H. Griesser, M. Eiselt, and J.-P. Elbers, "DMT modulation with adaptive loading for high bit rate transmission over directly detected optical channels," *J. Lightwave Technol.*, vol. 32, no. 21, pp. 4143–4153, Nov. 2014.
- [21] M. Bi, S. Xiao, H. He, J. Li, and Z. Zhou, "A new symbol timing synchronization scheme for direct modulation optical OFDM PON," in *Asia Communications and Photonics Conf. and Exhibition (ACP)*, Nov. 13–16, 2011.
- [22] R. A. Shafik, S. Rahman, and R. Islam, "On the extended relationships among EVM, BER and SNR as performance metrics," in *Int. Conf. on Electrical and Computer Engineering (ICECE)*, Dec. 19–21, 2006, pp. 408–411.
- [23] P. Golden, H. Dedieu, and K. S. Jacobsen, *Fundamentals of DSL Technology*. Taylor & Francis, 2005 [Online]. Available: <http://books.google.fr/books?id=m77kZl71gysC>.
- [24] G. P. Agrawal, *Nonlinear Fiber Optics*, 4th ed. San Diego, Academic, 2007.

- [25] J. M. Tang and K. A. Shore, "30-Gb/s signal transmission over 40-km directly modulated DFB-laser-based single-mode-fiber links without optical amplification and dispersion compensation," *J. Lightwave Technol.*, vol. 24, no. 6, pp. 2318–2327, June 2006.
- [26] C.-C. Wei, "Small-signal analysis of OOFDM signal transmission with directly modulated laser and direct detection," *Opt. Lett.*, vol. 36, pp. 151–153, 2011.



**Max Frejus Sanya** received his Dipl.-Ing. degree (first class honors) in signal processing of electrical engineering from Ecole Polytechnique d'Abomey-Calavi (EPAC), Benin, in 2008. He received his M.Phil. degree (first class honors) in electronics and telecommunication engineering from EPAC at the University of Abomey-Calavi (UAC), Benin, in 2010. He is currently at the end of his Ph.D. degree at XLIM Laboratory (University of Limoges, France) in cooperation with

the Laboratory of Electrical Telecommunication and Computer Applications (LETIA) at UAC, Benin. His research interests include wired/wireless signal processing and optical communications with focus on the following topics: next-generation PON transmission technology, channel estimation, dynamic resource allocation, peak-to-average power ratio (PAPR) reduction, and cost-effective high-speed optical transmission.



**Leopold Djogbe**, a holder of a Ph.D. in electronics since June 2000, is a research professor at the University of Abomey-Calavi (UAC-EPAC). As academic activities, he is currently deputy director of the Informatics and Telecommunications Engineering Department and supervises the work of engineers and M.Phil. degree holders in EPAC. On average per year, he participates in twenty boards on topics in electronics, telecommunication networks, and computer

science. In terms of scientific research, he is member of the Research Unit "Radio Frequency and Transmission" in the Electrotechnical Laboratory of Applied Informatics and Telecommunications (LETIA) and gets his publication credits from newspapers and participation in scientific conferences of both Abomey-Calavi and sub-regional universities. His interests are focused on the study of the impact of components on the performance of an optical transmission system, integration of digital techniques of signal

processing in optical communication, radio over fiber, and optoelectronics device characterization.



**Antoine Vianou** received his engineering Ph.D. and Es Sciences Ph.D. degree in energy with congratulations and honorable mention from the Higher Polytechnic School of the University of Dakar. He is currently a Full Professor of the Universities in Science and Technology Engineering, and was the first Beninese to reach the CAMES award degree. Among academic activities, he was Head of Postgraduate Studies and Research at Ecole Polytechnique d'Abomey-Calavi

(EPAC) in Benin until 2007; Permanent Secretary of the scientific committee sector "Science and Technology" of Abomey-Calavi University (UAC), Benin; and also a member of the standing committee of experts in charge of the third degree cycles and equivalency in the UAC. He has supervised 75 M.Phil. degrees and 25 Ph.D. students. He is author and co-author of numerous scientific publications in many scientific fields, such as thermophysics characterization of materials, renewable energy and thermal comfort of the home, and power electronics and telecommunications. He is also an expert in the Agence Universitaire de la Francophonie and instructor of applications of the African and Malagasy Council for Higher Education (CAMES). His interests are focused on many African network projects for teaching and research in the telecommunications field, and with energy and the environment.



**Christelle Aupetit-Berthelemot** received the engineer degree in telecommunication from Ecole Nationale Supérieure d'Ingénieurs de Limoges (ENSIL) in 1995. She received the M.S. degree as well as the Ph.D. degree in High Frequency and Optic Telecommunications from the University of Limoges, respectively, in 1995 and 1998. She obtained her accreditation to supervise research (Habilitation) in December 2006. She is currently a Professor at the University of Limoges and the Head of the Electronics and Telecommunications Department at ENSIL. She has been involved in several Cooperative Projects. Her current research activities concern optical telecommunication. Particularly, her interests are focused on the study of the impact of the components on the performance of optical transmission systems, integration of digital techniques of signal processing in optical communication, radio over fiber, and optoelectronics device characterization.

of Limoges and the Head of the Electronics and Telecommunications Department at ENSIL. She has been involved in several Cooperative Projects. Her current research activities concern optical telecommunication. Particularly, her interests are focused on the study of the impact of the components on the performance of optical transmission systems, integration of digital techniques of signal processing in optical communication, radio over fiber, and optoelectronics device characterization.